Quantum and classical localization and the Manhattan lattice

E J Beamond[1], **A L Owczarek**[2] **and J Cardy**[1,3]

[1] Theoretical Physics, University of Oxford, 1 Keble Road, Oxford OX1 3NP, UK
[2] Department of Mathematics and Statistics, University of Melbourne, Victoria, 3010, Australia
[3] All Souls College, Oxford, UK

Abstract
We consider a network model, embedded on the Manhattan lattice, of a quantum localization problem belonging to symmetry class C. This arises in the context of quasiparticle dynamics in disordered spin-singlet superconductors which are invariant under spin rotations but not under time reversal. A mapping exists between problems belonging to this symmetry class and certain classical random walks which are self-avoiding and have attractive interactions; we exploit this equivalence, using a study of the classical random walks to gain information about the corresponding quantum problem. In a field-theoretic approach, we show that the interactions may flow to one of two possible strong-coupling regimes separated by a transition: however, using Monte Carlo simulations we show that the walks are in fact always compact two-dimensional objects with a well-defined one-dimensional surface, indicating that the corresponding quantum system is localized.

PACS numbers: 72.15.Rn, 05.40.Fb, 64.60.Ak, 05.50.+q

1. Introduction

Disordered electronic systems, and the associated metal–insulator transitions, have generated much interest in recent years. In this paper, we consider a two-dimensional system of non-interacting particles which is invariant under spin rotations but not under time reversal. According to the classification set out by Altland and Zirnbauer [1] such a system belongs to symmetry class C. This class is one of several which are distinct from the three Wigner–Dyson classes and have realizations as Bogoliubov–de Gennes Hamiltonians for quasiparticles in disordered superconductors. In particular, class C arises in spin-singlet superconductors with broken time-reversal symmetry for orbital motion but negligible Zeeman splitting [1].

For two-dimensional systems with broken time-reversal symmetry, whether from the Wigner–Dyson unitary class or from class C, there exists the possibility of a delocalization
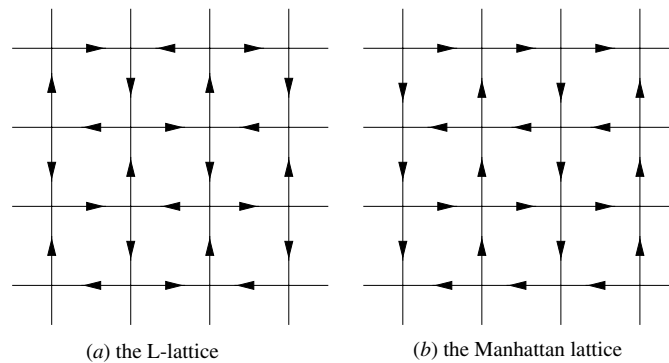
(*a*) the L-lattice　　　　　　　　　　(*b*) the Manhattan lattice

Figure 1. The L-lattice and Manhattan lattice.

transition of the quantum Hall type. Recent studies of network models for systems belonging to class C [2–7] have focused on this transition, yielding several interesting results. Notably, one such network model describes the spin quantum Hall effect, with two insulating phases separated by a delocalization transition analogous to the quantum Hall plateau transition. The two phases exhibit quantized Hall conductance differing by an integer. It has been shown [4, 7] that this quantum problem may be mapped to that of the hulls of classical percolation clusters in two dimensions, a well-understood problem. The particular network model used in these studies was based on the L-lattice (see figure 1(*a*)), and is a natural generalization of the Chalker–Coddington model [8] which was designed to study the ordinary integer quantum Hall transition.

The L-lattice is a square lattice consisting of directed edges and nodes, such that every path following the directed edges must turn left or right at each node. It possesses a particular symmetry under inversion about a diagonal axis which reflects the symmetry of the corresponding quantum hamiltonian about a particular energy.

However, in [7] it was shown that the mapping of network models in class C to classical random walk models is more general, and holds on any directed lattice (at least if each node is of degree 4.) These walks are in general *trails*, in that they may not pass over a given link more than once, but they also have attractive interactions at each node. In the mapping, localized and extended phases of the quantum system map to regions of parameter space where the corresponding classical walks either close after a finite number of steps (almost surely) or they escape to infinity. The localization behaviour exhibited by a given network model and the nature of the corresponding classical problem are expected to be strongly dependent on the structure of the underlying lattice. Therefore, by studying classical problems formulated on different lattices, we might uncover different types of localization behaviour, resulting in the competition between the edge exclusion and nodal attraction.

The classical random walks in which we are interested, together with other kinetic self-avoiding trails, correspond to the classical scattering of light by random arrays of mirrors laid out on a square lattice. Problems of this type have been studied extensively [9–12]. These processes may also be viewed as history-dependent kinetic random walks. For example, in terms of the mirror model, the walker lays down a mirror at random on visiting a node; on return to that node, it finds the mirror already fixed there. Therefore, models of this type may be classified as 'true' self-avoiding walks. This class of walks has been studied in the limit of weak scattering using field-theoretic renormalization group methods [13–15]; we shall make

use of such techniques in section 2 of this paper to study such walks. We note that, as for Anderson localization, the critical dimension for these processes is 2.

As mentioned above, the network model describing the spin quantum Hall effect is formulated on the L-lattice (figure 1(a)). In the heuristic justification for studying this lattice in this context (and for the original Chalker–Coddington model) it is seen as a distorted version of a random lattice, whose plaquettes correspond to the regions where locally either $E - V$ is <0 or >0, where E is the Fermi energy and V is some slowly varying random potential. In the semi-classical approximation, there are edge states propagating along the curves which divide these regions. Along these, the quasiparticle wavefunction suffers a constant spin (or phase) rotation. On distorting the random geometry to the L-lattice, these become quenched random link variables of the model.

In this paper, we consider a different lattice, the Manhattan lattice. It shares with the L-lattice the property that at each node there are two incoming and two outgoing edges or links, so that the theorems of [7] apply. On this lattice, a walker may either continue straight on at a given node with a given probability or make a turn. The allowed directions for turning at each node alternate right and left, as shown in figure 1(b). The overall lattice is therefore regular, with a similar size unit cell to the L-lattice. In the network model, at each node there is a real unitary S-matrix which describes scattering from the incoming edges to the outgoing ones. Just as for the models on the L-lattice, this is in principle also a quenched random matrix, but for simplicity we shall take it to be the same at all nodes. Thus the S-matrix elements for continuing straight on at each node are taken to be $\cos \theta$, and those for turning are $\pm \sin \theta$. When $\cos \theta = 1$, the quasiparticles move ballistically along the lattice axes, while for $\sin \theta = \pm 1$ they move around the perimeter of single plaquettes. The existence of a ballistic limit distinguishes this lattice from the L-lattice. On the other hand, the Manhattan lattice appears to enjoy no special symmetry, as does the L-lattice about $\theta = \pi/4$.

The general results of [7] show that the single-particle Green's function and the two-point conductance for a class C model on this lattice are related to the properties of classical trails, or random walks which visit each edge no more than once, and, on first visiting a given node, turn L (left) or R (right) with probability $p \equiv \sin^2 \theta$, or continue straight with probability $1 - p = \cos^2 \theta$. For the L-lattice, the limits $p \to 0$ and $p \to 1$ show clearly two distinct behavioural phases, characterized by different edge states; a delocalization transition occurs at $p = \frac{1}{2}$. For the model formulated on the Manhattan lattice, however, we might expect to find different behaviour, since it is clear that there are no corresponding edge states as $p \to 0, 1$. We note also that a kinetic self-avoiding trail on the Manhattan lattice may cross itself with probability p, but this is never permitted on the L-lattice.

At $p = 1$, the walks are simply loops defining the elementary plaquettes of the lattice. In fact, it may be argued [16] that the trajectories are loops of finite extent at least for $p > \frac{1}{2}$: if we place a mirror at $45°$ at each of the vertices where the path turns through $\pm 90°$, they may be thought of as forming clusters of bonds on a square lattice at $45°$ to the original. For $p > \frac{1}{2}$ the mirrors percolate: that is, they form an infinite cluster which crosses the entire lattice, with probability 1. The trajectories are confined to the voids in this cluster, which are finite. For $0 < p \leqslant \frac{1}{2}$, this argument is inconclusive: the trajectories will scatter from the finite clusters of mirrors, but this may or may not lead to classical localization. At $p = 0$ all trajectories are straight lines; the states to which they correspond are spatially extended. Therefore either almost all trajectories are localized for all $p > 0$, or there is a transition at some finite value $0 < p_c \leqslant \frac{1}{2}$ from extended to localized behaviour.

In this paper, we use two approaches to study the kinetic processes described above. In section 2, we develop a field-theoretic description of the weak-coupling regime of this particular type of 'true' self-avoiding walk. We begin by estimating the diffusion constant for

the Manhattan lattice, and show that the problem is in this regime as $p \to 0$. We then use field-theoretic renormalization group methods to analyse the general class of such problems: the RG trajectories always run away from the weak-coupling fixed point, with possibility of two distinct strong-coupling behaviours separated by a critical trajectory. However, in section 3, we use Monte Carlo methods directly to simulate kinetic self-avoiding trails on the Manhattan lattice. These simulations are only practical for values of p larger than about 0.2. However, they all indicate that the walks are localized, with a mean length and spatial extent which decrease with increasing p. These numerical results thus complement those of section 2. In addition to their relevance to the corresponding quantum localization problem, these classical processes are of interest in their own right. In section 4, we discuss possibilities for related future work.

2. Analytic results

2.1. Estimation of the diffusion constant

As a first step in analysing the weak-interaction limit of this model, we estimate the diffusion constant of a random walker on the Manhattan lattice, subject to no restrictions on return to the same node or link. A diffusive path $\mathbf{r}(t)$ which takes a step of finite length at each unit time exhibits the behaviour

$$\langle [\mathbf{r}(t) - \mathbf{r}(0)]^2 \rangle = 4Dt \qquad (2.1)$$

where the lattice-dependent quantity D is the diffusion constant. For convenience, we shall take $\mathbf{r}(0) = \mathbf{0}$ in what follows. The diffusion constant for a given random walk may be calculated by recasting the position coordinates of points visited on the path as a sum r_t of complex numbers,

$$r_t = z_1 + z_2 + \cdots + z_t \qquad (2.2)$$

where $z_{j+1} = z_j \, e^{i\theta_j}$. For the random walks in which we are interested, we require additionally $|z_j| = a$ for all j, where a is the lattice bond length. The distribution of θ_j depends on the details of the lattice; the θ_j are assumed to be uncorrelated, so that each step of the random process is independent of all previous history. For the Manhattan lattice, the distribution for the θ_j is somewhat complicated because the allowed turning directions at a given node are dependent upon the position of the node on the lattice. For turning probability p, the mean free path of a particle moving randomly on the Manhattan lattice $\tau_{\mathrm{mfp}} \sim 1/p$; hence for small p, $\tau_{\mathrm{mfp}} \gg 1$. We therefore assume that the particle is unable, on the length scale of the mean free path, to tell whether it will next change direction at a left-turn or right-turn node. Thus the options of turning left or right are assigned equal probability in this approximation. The corresponding distribution for θ_j is

$$\theta_j = \begin{cases} 0 & \text{with probability } 1 - p \\ -\pi/2 & \text{with probability } p/2 \\ +\pi/2 & \text{with probability } p/2 \end{cases} \qquad (2.3)$$

with angles measured in an anti-clockwise direction. Thus $\langle e^{i\theta_j} \rangle = 1 - p + e^{i\pi/2} p/2 + e^{-i\pi/2} p/2 = 1 - p$ for all j, and $\langle e^{i(\theta_1 + \cdots + \theta_r)} \rangle = \langle e^{i\theta_1} \rangle^r = (1 - p)^r$. Now from (2.2), we have

$$r_t = z_1(1 + e^{i\theta_1} + \cdots + e^{i(\theta_1 + \cdots + \theta_{t-1})}). \qquad (2.4)$$

Hence, since $\langle |\mathbf{r}(t)|^2 \rangle \equiv \langle r_t r_t^* \rangle$,

$$\langle |\mathbf{r}(t)|^2 \rangle = |z_1|^2 ((2 - p)p^{-1}t - 2(1 - p)p^{-2}(1 - (1 - p)^t)). \qquad (2.5)$$

At large t, $(1 - p)^t \to 0$, yielding

$$\langle |\mathbf{r}(t)|^2 \rangle \approx |z_1|^2 ((2 - p) p^{-1} t - 2(1 - p) p^{-2}). \tag{2.6}$$

Thus for the Manhattan lattice,

$$D \approx (2 - p) p^{-1}. \tag{2.7}$$

We note that at $p = 0$, the diffusion constant becomes infinite; this characterizes superdiffusive behaviour. In this particular example of superdiffusion, we also find that the mean square displacement $\langle [\mathbf{r}(t) - \mathbf{r}(0)]^2 \rangle$ diverges faster than linearly with time. In fact, it is easy to see that $\langle [\mathbf{r}(t) - \mathbf{r}(0)]^2 \rangle = a^2 t^2$ since for $p = 0$ the random walk proceeds in a straight line. We therefore see a transition to a different kind of behaviour exactly at $p = 0$.

2.2. A field-theoretic approach

2.2.1. Peliti's field theory for true self-avoiding walks.
The starting point for our renormalization group approach is the field-theoretic description proposed by Peliti [13–15] for the class of true self-avoiding walks to which our bond-avoiding paths on the Manhattan lattice belong. The theory is composed of two scalar fields $\tilde{\psi}(\mathbf{r}, t)$ and $\psi(\mathbf{r}, t)$, which respectively create and destroy walks. The Hamiltonian $\mathcal{H}$ is given by $\mathcal{H} = \mathcal{H}_0 + \mathcal{H}_I$, where $\mathcal{H}_0$ is the 'free' Hamiltonian

$$\mathcal{H}_0 = \int_0^\infty dt \int d^d \mathbf{r} \, \tilde{\psi}(\mathbf{r}, t) \left[-\frac{\partial}{\partial t} + D\nabla^2 \right] \psi(\mathbf{r}, t) \tag{2.8}$$

and $\mathcal{H}_I$ is an interaction Hamiltonian whose precise form depends on the nature of the process under consideration. D represents the bare diffusion constant, as computed above. From this class of Hamiltonians arise well-defined Feynman rules for the theory. The correlation function $G(\mathbf{r}, t) = \langle \tilde{\psi}(0, 0) \psi(\mathbf{r}, t) \rangle$ yields the probability density for a walk beginning at the origin to be found at position $\mathbf{r}$ after time t. After applying a Fourier transform to the spatial components of $G(\mathbf{r}, t)$ and a Laplace transform to the temporal component, we obtain the bare propagator

$$\tilde{G}(\mathbf{p}, \mu) = \tilde{G}_0(\mathbf{p}, \mu) \equiv (\mu + Dp^2)^{-1}. \tag{2.9}$$

The generalized interaction contribution is given by

$$\gamma(\mathbf{p}, \mathbf{q}, \mathbf{p_1}) = (\mathbf{p_1} \cdot \mathbf{q}) g_1 + (\mathbf{p_1} \cdot (\mathbf{p_1} + \mathbf{q})) g_2 + (\mathbf{p_1} \cdot \mathbf{p}) g_3 \tag{2.10}$$

where $\mathbf{p}$ is the earliest incoming wavenumber and $\mathbf{p_1}$ is the latest outgoing wavenumber. The values of the couplings g_i depend on the nature of the random walk. For example, for Peliti's true self-avoiding walk, one should take $g_1 = g$ and $g_2 = g_3 = 0$; this corresponds to the interaction Hamiltonian

$$\mathcal{H}_I = -g \int_0^\infty dt \, dt' \int d^d \mathbf{r} \, (\psi(\mathbf{r}, t') \nabla \tilde{\psi}(\mathbf{r}, t')) \cdot (\psi(\mathbf{r}, t) \nabla \tilde{\psi}(\mathbf{r}, t)). \tag{2.11}$$

Since the coupling constants are dimensionless quantities, the upper critical dimension of this class of theories is $d_c = 2$. The general theory may be renormalized by dimensional regularization and minimal subtraction in two dimensions. Mass renormalization is trivial. However, the diffusion constant is renormalized by a factor Z so that $D = ZD_R$, and renormalized coupling constants are given by $u_i \kappa^\epsilon$, $i = 1, 2, 3$, where κ is the renormalization wavenumber. A calculation to order one loop gives diffusion constant renormalization factor

$$Z = 1 + \epsilon^{-1}(u_3 - u_1) \tag{2.12}$$

and renormalization group equations

$$\frac{du_1}{d\tau} = -\epsilon u_1 + \frac{5}{2}u_1^2 + \frac{1}{2}u_2^2 - 2u_1u_2 - 3u_1u_3 \tag{2.13}$$

$$\frac{du_2}{d\tau} = -\epsilon u_2 - u_1^2 - u_2^2 + 3u_1u_2 + u_1u_3 - 3u_2u_3 \tag{2.14}$$

$$\frac{du_3}{d\tau} = -\epsilon u_3 - \frac{5}{2}u_3^2 + 2u_1u_3 - u_2u_3 \tag{2.15}$$

where $\tau = \log(\kappa'/\kappa)$ is the logarithm of the scale parameter.

2.2.2. Constructing an interaction Hamiltonian. In order to apply these general results to the random walks in which we are interested, we now examine in detail the types of interaction which might arise for kinetic self-avoiding processes on the Manhattan lattice. There are two competing interactions involved: the node interactions are attractive, and clearly the bond interactions in this type of self-avoiding process must be repulsive. Thus one way to look at the effect of these interactions is to begin with a free kinetic walk on the Manhattan lattice and then introduce appropriate weights to model self-avoiding characteriztics. We impose a repulsive weight $\exp(-\beta V M(M-1)/2)$ (with $V > 0$) for every bond visited M times and an attractive weight $\exp(+\beta V' N(N-1)/2)$ (with $V' > 0$) for every node visited N times, and examine the resultant modification to the free kinetic walk. To work to first order in V and V', it is sufficient to consider only cases where a path has visited each node and bond on the lattice no more than twice.

On average, there is no directional bias to these processes on the Manhattan lattice; therefore, no drift terms, or equivalently no first-order gradient terms, should appear in the interaction Hamiltonian. However, higher order gradients may be obtained by examining the hopping terms generated as the particle moves on the lattice. These should respect the global rotational invariance of the kinetic walks. Consider, for example, a move from $\mathbf{r_1}$ to $\mathbf{r_2}$ at time t_2. This is effected by the probability-conserving term $\tilde{\psi}(\mathbf{r}_2)\psi(\mathbf{r}_1) - \tilde{\psi}(\mathbf{r}_1)\psi(\mathbf{r}_1)$. Note that the particle density at position $\mathbf{r}$ and time t is given by $\tilde{\psi}(\mathbf{r}, t)\psi(\mathbf{r}, t)$, and takes values 0 or 1. Now suppose that the midpoints of the exit bonds at a particular node have position vectors $\mathbf{r}_i$, with $i = 1, \ldots, 4$. Thus to describe a first visit to the node at time t_1 and a subsequent visit at time t_2, approaching from $\mathbf{r}_1$ and leaving via $\mathbf{r}_2$, we postulate an interaction term of the form

$$[\tilde{\psi}(\mathbf{r}_2, t_2)\psi(\mathbf{r}_1, t_2) - \tilde{\psi}(\mathbf{r}_1, t_2)\psi(\mathbf{r}_1, t_2)]\sum_{i=1}^{4}\alpha_i\tilde{\psi}(\mathbf{r}_i, t_1)\psi(\mathbf{r}_i, t_1) \tag{2.16}$$

with the α_i appropriately chosen to give the correct Boltzmann weights. Suppose that the possible routes through a given node are $\mathbf{r_1} \rightarrow \mathbf{r_2}, \mathbf{r_1} \rightarrow \mathbf{r_3}, \mathbf{r_4} \rightarrow \mathbf{r_2}$ and $\mathbf{r_4} \rightarrow \mathbf{r_3}$. Then applying weights V and V' as defined above, if the path passes from $\mathbf{r_1}$ to $\mathbf{r_2}$ on both visits to the node, we obtain

$$\alpha_1 + \alpha_2 = -2V + V'. \tag{2.17}$$

Considering each of the other possible routes through the node, we find alsoM

$$\alpha_1 + \alpha_3 = -V + V' \tag{2.18}$$

$$\alpha_2 + \alpha_4 = -V + V' \tag{2.19}$$

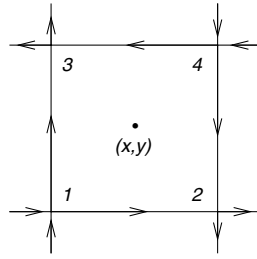$$\alpha_3 + \alpha_4 = +V'. \tag{2.20}$$

Figure 2. A unit cell on the Manhattan lattice with centre at the point (x, y); the possible node types are labelled 1 to 4. Each lattice bond has length $2a$.

We therefore have a set of simultaneous equations for the α_i. Note that these are invariant under the transformation $\alpha_{1,4} \to \alpha_{1,4} + A$, $\alpha_{2,3} \to \alpha_{2,3} - A$ for any A, so that there is always some arbitrariness in the solutions. However, if $V' = 0$, i.e. there is no node interaction, then $\alpha_1 = \alpha_2 = -V$, $\alpha_3 = \alpha_4 = 0$ is a solution. Similarly, if $V = 0$, i.e. there is no bond interaction, then $\alpha_1 = \alpha_2 = \alpha_3 = \alpha_4 = V'/2$ is a solution. We thus obtain bond interactions of the form

$$-V(\tilde{\psi}(\mathbf{r_j}, t_2)\psi(\mathbf{r_i}, t_2) - \tilde{\psi}(\mathbf{r_i}, t_2)\psi(\mathbf{r_i}, t_2))(\tilde{\psi}(\mathbf{r_j}, t_1)\psi(\mathbf{r_i}, t_1) + \tilde{\psi}(\mathbf{r_j}, t_1)\psi(\mathbf{r_j}, t_1)) \qquad (2.21)$$

and node interactions of the form

$$\frac{1}{2}V'(\tilde{\psi}(\mathbf{r_j}, t_2)\psi(\mathbf{r_i}, t_2) - \tilde{\psi}(\mathbf{r_i}, t_2)\psi(\mathbf{r_i}, t_2)) \sum_{\mathbf{r'} \in \text{node}} \tilde{\psi}(\mathbf{r'}, t_1)\psi(\mathbf{r'}, t_1) \qquad (2.22)$$

where, on the second visit, the path approaches the node from $\mathbf{r_i}$ and leaves via $\mathbf{r_j}$.

A unit cell on the Manhattan lattice contains four different node configurations, as illustrated in figure 2. In order to construct the interaction terms in the Hamiltonian then, we must compute the contribution for both node and bond interactions from each of the nodes in the unit cell. Consider, for example, node 1 in figure 2, positioned at $(x - a, y - a)$. A possible route through this node might arrive at the point $\mathbf{r_j} = (x - 2a, y - a)$ at time t_2 and leave via $\mathbf{r_i} = (x, y - a)$. The second-order gradient expansion for this hopping process is given by

$$\tilde{\psi}(\mathbf{r_j}, t_2)\psi(\mathbf{r_i}, t_2) - \tilde{\psi}(\mathbf{r_i}, t_2)\psi(\mathbf{r_i}, t_2)$$
$$= \tilde{\psi}(x, y - a, t_2)\psi(x - 2a, y, t_2) - \tilde{\psi}(x - 2a, y, t_2)\psi(x - 2a, y, t_2)$$
$$= 2a\frac{\partial \tilde{\psi}_2}{\partial x}\psi_2 - 2a^2\frac{\partial^2 \tilde{\psi}_2}{\partial x^2}\psi_2 - 2a^2\frac{\partial^2 \tilde{\psi}_2}{\partial x \partial y}\psi_2 - 4a^2\frac{\partial \tilde{\psi}_2}{\partial x}\frac{\partial \psi_2}{\partial x} - 2a^2\frac{\partial \tilde{\psi}_2}{\partial x}\frac{\partial \psi_2}{\partial y}.$$
$$(2.23)$$

In the last line above, the subscript 2 indicates time t_2 and the position argument (x, y) of the ψ, $\tilde{\psi}$ has been omitted for clarity. Combining the contributions for all the possible routes through each of the four nodes belonging to the unit cell, we obtain the node interaction term

$$-16\frac{V'}{2}a^2(3(\nabla\tilde{\psi}(\mathbf{r}, t_2) \cdot \nabla\psi(\mathbf{r}, t_2))(\tilde{\psi}(\mathbf{r}, t_1)\psi(\mathbf{r}, t_1))$$
$$+ 4\nabla \cdot (\sigma_z(\nabla\tilde{\psi}(\mathbf{r}, t_2))\psi(\mathbf{r}, t_2)\tilde{\psi}(\mathbf{r}, t_1)\psi(\mathbf{r}, t_1))) \qquad (2.24)$$

and bond interaction term

$$8Va^2(3(\nabla\tilde{\psi}(\mathbf{r}, t_2) \cdot \nabla\psi(\mathbf{r}, t_2))(\tilde{\psi}(\mathbf{r}, t_1)\psi(\mathbf{r}, t_1))$$
$$+ 4\nabla \cdot (\sigma_z(\nabla\tilde{\psi}(\mathbf{r}, t_2))\psi(\mathbf{r}, t_2)\tilde{\psi}(\mathbf{r}, t_1)\psi(\mathbf{r}, t_1))) \qquad (2.25)$$

where σ_z is the Pauli matrix with entries $\sigma_{ij} = 1 - \delta_{ij}$. The interaction Hamiltonian may now be obtained by integrating over all position space and over t_1 and t_2 with $0 < t_1 < t_2$. Note that the total divergences in (2.24) and (2.25) simply yield a boundary term on integrating with respect to **r**. We therefore have

$$\mathcal{H}_I = -24(V' - V) \int d^d\mathbf{r} \int_0^\infty dt_2 \int_0^{t_2} dt_1 (\nabla\tilde{\psi}(\mathbf{r}, t_2) \cdot \nabla\psi(\mathbf{r}, t_2))(\tilde{\psi}(\mathbf{r}, t_1)\psi(\mathbf{r}, t_1)). \quad (2.26)$$

We see immediately, by comparison with the free Hamiltonian $\mathcal{H}_0$ in (2.8), that the effect of this interaction is only to modify the diffusion constant. Thus if the trail has already visited a particular region of the lattice, it will experience a change in diffusion speed when it revisits this region. The nature of the modification depends solely upon the relative values of the bond and node interaction strengths, through the factor $V' - V$. The interaction derived above leads to a coupling proportional to $\mathbf{p}_1 \cdot (\mathbf{p}_1 + \mathbf{q})$. Therefore, referring back to the generalized interaction term displayed in (2.10), we see that in order to obtain the correct coupling for the kinetic self-avoiding trail on the Manhattan lattice, we must choose initially $g_2 = O(V, V')$, and $g_1 = g_3 = O(V^2, V'^2, VV')$. This is in contrast to the kinetic self-avoiding trail considered by Peliti, for which $g_1 > 0$ and $g_2 = g_3 = 0$ at $t = 0$. We see from (2.26) that, in the Manhattan case, g_2 is proportional to $V' - V$, to first order.

2.2.3. Renormalization group flows.

If $g_3 = 0$ initially, then to first order, $u_3 = 0$ always. To simplify matters, we assume that this remains the case: this does not affect our qualitative conclusions. If we also choose $u_1 = 0$ initially, then from equation (2.12) we find that the diffusion constant renormalization factor $Z = 1$ at this point. This indicates that there is no singular contribution to the diffusion constant from the renormalization at weak coupling, and therefore the dynamic exponent $z = 2$, with the possible appearance of corrections from the strong-coupling behaviour; that is, time t scales as the square of the spatial extension $r = |\mathbf{r}(t)|$. From the analysis presented earlier in this section, in $d = 2$ dimensions the renormalization group equations for u_1 and u_2 in the $u_3 = 0$ plane are given by

$$\frac{du_1}{d\tau} = \frac{5}{2}u_1^2 + \frac{1}{2}u_2^2 - 2u_1u_2 \quad (2.27)$$

$$\frac{du_2}{d\tau} = -u_1^2 - u_2^2 + 3u_1u_2. \quad (2.28)$$

Hence the only fixed point for $\epsilon = 0$ is the trivial fixed point $u_1 = u_2 = 0$. This corresponds to the case $p = 0$, for which the trails are necessarily non-interacting. The renormalization group flow equations may be integrated to yield the general solution

$$u_1 - u_2 = A(u_1 + u_2)^{5/3}(2u_1 - u_2)^{1/3} \quad (2.29)$$

where if initially $u_1 = 0$ and $u_2 = u_2^0$, then $A = 1/u_2^0$. Much may be learned by examining these flow trajectories. Figure 3 illustrates schematically renormalization group flow in the plane $u_3 = 0$. The attractors $u_2 = Mu_1$ may be identified by dividing (2.27) by (2.28) and solving the resulting equation for M. There are three solutions: $u_2 = -u_1$, $u_2 = 2u_1$ and $u_2 = u_1$.

If asymptotically $u_2 = Mu_1$ for some M, then in this limit the renormalization group equations give $u_1, u_2 \sim \tau^{-1}$. The flows in the direction of decreasing τ in figure 3 should show the approach to asymptotic behaviour: see [15]. We observe that a trajectory starting at $u_1 \approx 0$ and $u_2^0 > 0$ flows to the line $u_2 = -u_1$, whereas a trajectory beginning at $u_1 \approx 0$ and $u_2^0 < 0$ flows to $u_2 = 2u_1$. In both cases, we obtain runaway with a flow to strong coupling. These two basins of attraction are divided by the separatrix $u_2 = u_1$, along which the flows
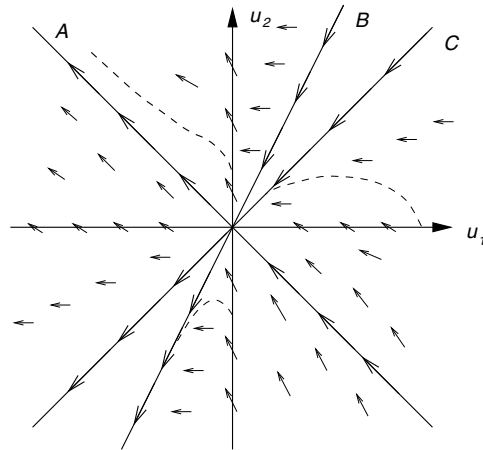
Figure 3. Schematic renormalization group flow diagram in the plane $u_3 = 0$. The arrows indicate the direction of decreasing τ, i.e. increasing κ. The three attractors are labelled (A) $u_2 = -u_1$, (B) $u_2 = 2u_1$ and (C) $u_2 = u_1$. Possible trajectories are illustrated schematically by dashed lines.

also go to strong coupling. Although in all three cases the flows go out of the region of validity of the one-loop approximation, nevertheless their topology is consistent with what we might expect for the phase diagram of trails with attractive on-site interaction, depending on the relative strengths of the bond repulsion V and the node attraction V'. Recall that, to first order, $u_2^0 \propto V - V'$. For $V \gg V'$ we would expect the walks to be in the universality class of trails, which is the same as that of ordinary self-avoiding walks [17, 18]. We may therefore interpret flows along the attractor $u_2 = -u_1$ as going towards a strong-coupling fixed point which corresponds to the universality class of self-avoiding walks (SAWs), even though this point is beyond the range of applicability of our analysis. Similarly, for $V' \gg V$ we might expect the walks to be collapsed, so that we may interpret the attractor $u_2 = 2u_1$ as flowing towards a (trivial) strong-coupling fixed point representing compact objects. Within this interpretation, then, flows along the separatrix go towards a strong-coupling fixed point corresponding to the collapse transition, that is the θ-point. (We note that for this simple phase diagram we need to assume that the initial value of u_1, computed to second order in V and V', is slightly negative, otherwise there will be an intermediate phase in which the flows go to weak coupling, as for the Peliti model.)

Although this analysis is based on a weak-coupling expansion, the topology of the consequent phase diagram should extend to strong coupling, unless there are further unexpected phase boundaries. It does not, however, tell us the form of the phase boundary for larger values of V and V', and in particular in which phase the original lattice model lies. Thus we turn to numerical simulations in the next section.

Although the flows in (2.27), (2.28) always go to strong coupling in our case, if we assume that they go to a fixed point describing a phase with a finite length scale ξ (for example the radius of gyration in the collapsed phase), we may still use them to predict the form of the dependence of ξ on the initial, weak-coupling, parameters. This is because the largest contribution comes from the neighbourhood of the weak-coupling fixed point. In general, any such length scale satisfies

$$\xi\left(u_2^0\right) = \xi_0 \exp\left(\int_0^{\tau^*} d\tau\right) \tag{2.30}$$

where ξ_0 is of the order of the microscopic cut-off, τ is the RG 'time', and τ^* is chosen so that $\xi(u_2(\tau^*)) = O(1)$. The integral here may be rewritten as

$$\int \frac{\mathrm{d}\tau}{\mathrm{d}u_2} \mathrm{d}u_2 = \int_{u_2^0}^{O(1)} \frac{\mathrm{d}u_2}{-u_1^2 - u_2^2 + 3u_1 u_2}. \tag{2.31}$$

Since initially $u_1 = O(u_2^2)$, the integral is $O(1/u_2^0)$ as $u_2^0 \to 0$, so that $\xi \sim \exp(1/u_2^0)$. This result would be academic were it not for the fact that the diffusion constant behaves as p^{-1} as $p \to 0$, and this places us squarely in the weak-coupling regime. Denoting the dimensionality of a quantity A by $[A]$, we find from (2.8) that $[\tilde{\psi}(\mathbf{r}, t)\psi(\mathbf{r}, t)] = k^d$ and $[D] = \mu k^{-2}$, where μ is the Laplace-transformed temporal variable and k represents momentum. From (2.26), we see that $[g_2]k^{2d}k^2 = \mu^2 k^d$, i.e. $[g_2] = \mu^2 k^{-d-2}$. Hence $g_2 \sim D^2 k^\epsilon$. Therefore the renormalized, dimensionless coupling $u_2 \sim g_2 D_R^{-2}\kappa^{-\epsilon}$. Now since, from section 2.1, the bare diffusion constant $D \sim p^{-1}$, we have $u_2^0 \sim p^2$. This leads to the leading order prediction $\xi \sim \mathrm{e}^{\mathrm{const}/p^2}$: the correlation length increases exponentially with decreasing p^2. This is entirely consistent with the only critical point of the lattice model being at $p = 0$.

3. Simulations

3.1. Preliminaries

In this section, we use Monte Carlo simulations to study various characteriztics of kinetic self-avoiding processes on the Manhattan lattice. The lattice bond length is chosen to be two units, so that $a = 1$ in the analysis above, and the lattice size is effectively infinite. The walker moves from one bond centre to an allowed neighbouring bond centre at each step, subject to the lattice bond directions and the condition that the path be self-avoiding; the number of steps taken is denoted by N. Thus a path consisting of one step, for which $N = 1$, connects two adjacent bond centres and has end-to-end length two units. Each simulation consists of a batch of 10^5 walks, which are grown individually. When a walk reaches the specified maximum length or closes, that is, returns to its initial coordinates, it is terminated and a new walk is started; in this way, the walks sampled at a given length N should be statistically independent. Data points for different values of N are generated from separate simulation runs. Errors on each data point are calculated as the variance of the quantity in question. Where curves have been fitted to the data, the fitting procedure employed an implementation of the nonlinear least-squares (NLLS) Marquardt–Levenberg algorithm.

3.2. Survival probability

Survival probability $P(N)$ is defined as the proportion of simulated paths which have not yet closed after the Nth step. This is expected to be a p-dependent quantity: at $p = 1$, $P(N) = 0$ for $N \geqslant 4$, and at $p = 0$, $P(N) = 1$ for all N as the trails simply proceed straight along a given direction. The data plotted in figure 4 suggest that $P(N)$ decays exponentially with increasing N, on a p-dependent length scale. This corresponds to localization for all non-zero p. Since all paths are extended at $p = 0$, this provides evidence in support of the existence of a trivial critical point, as discussed earlier. In fact, we find that the simulated values for survival probability are consistent with a scaling form given by

$$P(N/N^*, p) \sim \mathrm{e}^{-N/N^*(p)} \mathrm{e}^{-C(p)\sqrt{N/N^*(p)}} \tag{3.1}$$

where $N^*(p)$ may be interpreted as the typical number of steps taken by a path before closure. Estimated values for $C(p)$ and $N^*(p)$, obtained by fitting the scaling form of (3.1) to the
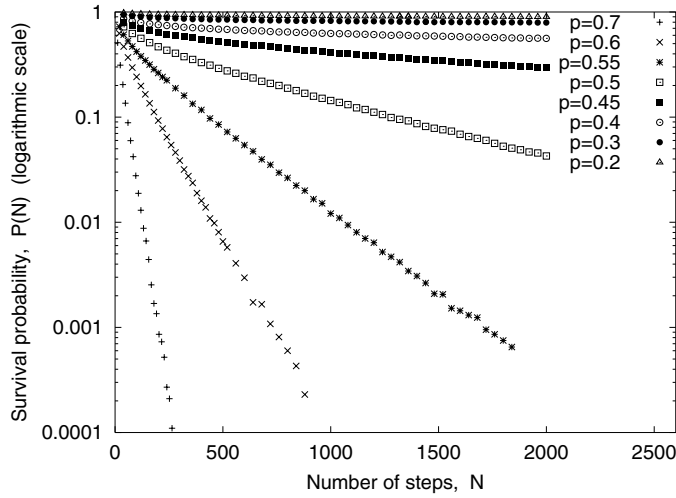
Figure 4. Survival probability as a function of path length, plotted for various p. Maximal values for N are: $p = 0.7$, $N_{max} = 264$; $p = 0.6$, $N_{max} = 880$; $p = 0.55$, $N_{max} = 1840$; $p \leqslant 0.5$, $N_{max} = 2000$. The vertical axis carries a logarithmic scale.

Table 1. Values for coefficient $C(p)$ and typical path length $N^*(p)$, tabulated for various p. Accuracy is to 3SF.

p	$N^*(p)$	$C(p)$
0.7	34.0	0.346
0.6	158	1.15
0.55	338	0.748
0.5	1320	1.23

simulated data, are presented in table 1 for certain values of p. Note that the typical length N^* increases as p decreases; for this reason, it was found to be extremely difficult to obtain reliable estimates for $N^*(p)$ and $C(p)$ for $p < 0.5$. Indeed, at $p < 0.5$ it is not possible to give reliable estimates for N^* since the estimated values are larger than the maximal value of N used in the simulations. However, this is to be expected since as $p \to 0$, N^* should tend to infinity. Figure 5 shows rescaled data $A(p)^{-1}P(N/N^*, p)\exp(C(p)\sqrt{N/N^*(p)})$ plotted against $N/N^*(p)$, where $A(p)$ is the normalization factor required for (3.1). The data collapse on to the line $f(N/N^*) = \exp(-N/N^*)$, also plotted in figure 5, showing excellent agreement with the postulated scaling equation. Note that since the typical length scale for closure of walks is much longer for smaller values of p, as predicted in the final part of section 2.2, data for these simulations are plotted over a smaller range of N/N^*. The scaling behaviour of (3.1) may be justified by the following argument, which is motivated partially by evidence presented in section 3.4 for scaling of internal energy.

The kinetic self-avoiding processes in which we are interested are non-equilibrium problems. However, it is possible to use statistical mechanics to examine their structure by exploiting an equivalence with certain equilibrium objects. To demonstrate this equivalence, we employ arguments similar to those used by Bradley for kinetic growth walks on the Manhattan lattice [19, 20] and by Owczarek and Prellberg for trails on hypercubic lattices [21, 22]. Consider an equilibrium model whose configurations are kinetic self-avoiding trails
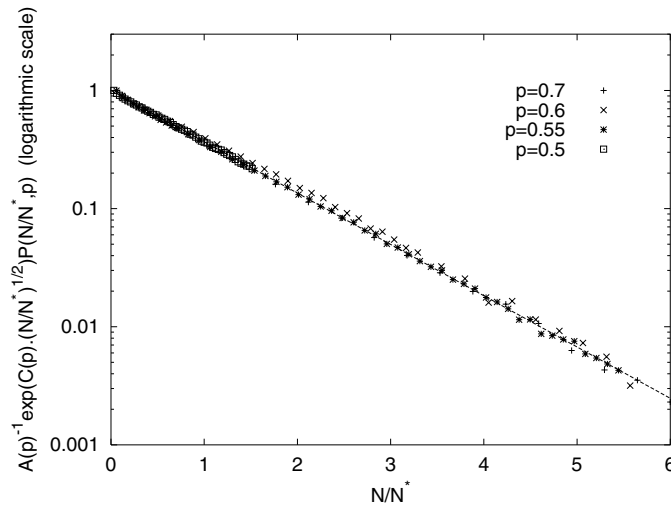
Figure 5. Rescaled data for survival probability, taking the form $A(p)^{-1}P(N/N^*, p)$ $\exp(C(p)\sqrt{N/N^*(p)})$, are plotted against the rescaled path length N/N^* for selected values of p. The dashed line shows $f(N/N^*) = \exp(-N/N^*)$.

laid down on the Manhattan lattice. For the moment, we look only at the case $p = \frac{1}{2}$. The temperature is fixed at a particular value, as is usual with Monte Carlo simulations. Now suppose that each doubly occupied node on a trail is assigned a weighting w. If $w = 1$, then this weighting will simply yield ordinary trails, on which a node may be visited any number of times. However, if w is large then the path should be a highly compact object. For our kinetic self-avoiding trails, the appropriate weighting is $w = 2$: when the path arrives at a node for the first time, it may choose either of two possible exits, with probability $p = \frac{1}{2}$ of making each choice, but on revisiting the node, the path must leave by the one unoccupied exit with probability 1. Let $\phi(N)$ be an open path configuration with length N steps, on which $n(\phi)$ nodes are doubly occupied. The probability of obtaining this configuration is $p_{\phi(N)} = (1/2)^{N-n(\phi)}$. However, as we have seen, there is also the possibility of generating a path which is a closed loop; the probability $P(N)$ of obtaining an open configuration at length N is less than 1. In fact,

$$P(N) = \sum_{\phi(N)} p_{\phi(N)} = 2^{-N} \sum_{\phi(N)} 2^{n(\phi)} = 2^{-N} \mathcal{Z}_N(2) \tag{3.2}$$

where $\mathcal{Z}_N(2)$ is the partition function for the equilibrium model, with the Boltzmann weight $w = 2$. Thus the set of kinetic self-avoiding growth trails at $p = \frac{1}{2}$ is a sample from the Boltzmann distribution of equilibrium trails with weighting $w = 2$. Further, the mean number of doubly occupied nodes is given by $w\, \mathrm{d}F/\mathrm{d}w$ evaluated at $w = 2$, where F is the free energy of the equilibrium model. This relationship is particularly useful since the mean number of doubly occupied nodes may readily be computed from simulations.

For a free random walk, $\mathcal{Z}_N = 4^N$, where N is the number of steps taken, since the walker may leave a given node via any of the four associated bonds. Thus, in this case, $F \sim N \log 4$. Note that since the bulk fractal dimension of a walk model is given by $d_f = 1/\nu$, where the radius of gyration scales with exponent ν, here $d_f = 2$. However, the free random walk does not have a well-defined surface. In contrast, there are other types of walk for which a surface may be identified. For collapsed polymers, for example, which may be modelled by certain

varieties of compact walk, a term appears in the partition function $\mathcal{Z}$, and hence also in the free energy F which scales according to the surface area of the object [23]. For an object embedded in d dimensions, the average extension in any given spatial direction is given by $R \sim N^{1/d}$, since $\nu = 1/d$. Therefore the surface area must scale as $R^{d-1} \sim N^{(d-1)/d}$. Thus in two dimensions, the surface area of a compact object scales like $N^{1/2}$. This leads to an expression of the free energy of the form

$$F \sim N F_b + N^{1/2} F_s + \cdots \tag{3.3}$$

where the $\cdots$ indicates smaller correction terms, and F_b and F_s are respectively bulk and surface contributions to the free energy. Hence the partition function must scale as

$$\mathcal{Z}_N(2) \sim \exp(N F_b + N^{1/2} F_s + \cdots). \tag{3.4}$$

From (3.2), we may therefore deduce that if the kinetic self-avoiding trails behave as compact walks, the probability of finding an open configuration after N steps should scale as

$$P(N) \sim \exp(N \log 2 + N F_b + N^{1/2} F_s + \cdots). \tag{3.5}$$

This is consistent with the scaling form of (3.1) which was fitted to the simulated data, suggesting that the kinetic self-avoiding trails are compact objects. It follows from our postulation of a trivial critical point that the scaling form (3.5) put forward for the case $p = \frac{1}{2}$ should hold for all non-zero p.

We note that our results indicate that kinetic growth trails on the Manhattan lattice are mapped to a temperature inside the collapsed phase of the equilibrium model. Previous kinetic growth models of walks and trails [19–22] in two and higher dimensions have all mapped to temperatures in the extended phase or θ-point of the corresponding equilibrium model. This makes our kinetic growth model of interest from the point of view of polymer models.

3.3. Radius of gyration and end-to-end distance

In this section we consider scaling of the spatial extension of the kinetic self-avoiding trails. We begin by examining the mean square radius of gyration, $\langle R_G^2 \rangle$, which is expected to scale as $N^{2\nu}$, for some ν. For a non-interacting random flight, $\nu = \frac{1}{2}$: $\langle R_G^2 \rangle = N a^2 (1 - N^{-2})/6$, where a is the (constant) step length [24]. It is also known that $\nu = 1/d$ for collapsed polymers in d dimensions. Figure 6 shows simulated data for trails which are still open after N steps. On fitting a scaling form $\langle R_G^2 \rangle = A(p) N^{2\nu(p)}$ to each dataset, we find that the estimated values for the exponent ν lie in the range $0.47 \lesssim \nu \lesssim 0.52$. Of course since the trails can never visit any bonds twice one can easily show that $\nu \geqslant \frac{1}{2}$. We have also studied the mean square radius of gyration for walks which close at the Nth step; the simulated data support a scaling form $\langle R_G^2 \rangle \sim N$, although the statistics obtained from these walks are not high. For example, for closed trails at $p = 0.5$, we have approximately $\langle R_G^2 \rangle \propto N^{1.05}$. This evidence strongly suggests that for both open and closed trails, $\langle R_G^2 \rangle \sim N^{2\nu}$ with $\nu = \frac{1}{2}$. This implies that the trails should be classified either as non-interacting random flights (polymer chains) or as compact walks (polymers in the collapsed phase) since both these have $\nu = \frac{1}{2}$ in two dimensions. However, evidence from the previous section suggests that the compact hypothesis is the most consistent one.

We next consider the scaling of end-to-end distance R_e for the trails. For the free random flight model, $\langle R_e^2 \rangle = N a^2$, where, as before, the step length is given by a. Thus for large N, $\langle R_G^2 \rangle \sim \langle R_e^2 \rangle / 6$ in this model. For compact walks, however, there should be corrections to this scaling form which result in suppression of the end-to-end distance relative to the non-interacting case. Figure 7 shows simulated data for the root mean square end-to-end distance $\sqrt{\langle R_e^2(N) \rangle}$ for trails at various values of p. Since this quantity does not
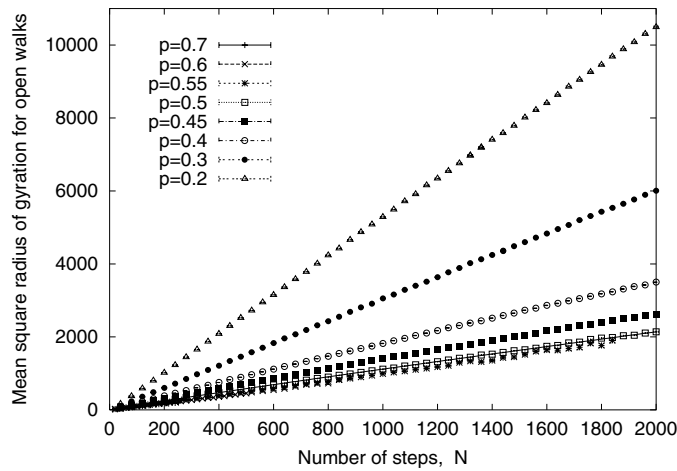
Figure 6. Scaling of mean square radius of gyration $\langle R_G^2 \rangle$ for open trails sampled after N steps. Data are plotted for p between 0.2 and 0.7. The line fitted to the data for $p = 0.5$ has equation $\langle R_G^2 \rangle \propto N^{0.94}$, where the exponent is quoted to two significant figures.
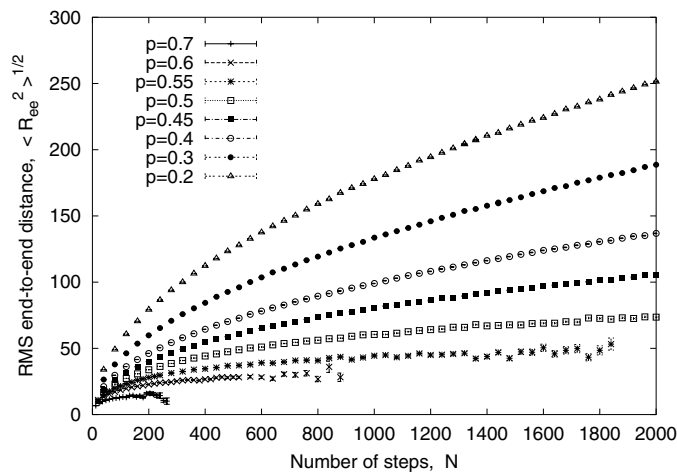

Figure 7. Scaling of RMS end-to-end distance with number of steps, for open trails, at various p. A line fitted to the data for $p = 0.5$ has equation $\langle R_e^2 \rangle \approx 0.104N + 135N^{1/2} - 728$, showing linear scaling with corrections $O(N^{1/2})$.

make sense for paths which have closed, the average is taken only over those paths which are still open after the Nth step. We find that the data are consistent with a scaling form $\sqrt{\langle R_e^2(N) \rangle} \sim N^{2\nu}(1 + BN^{-1/2} + CN^{-1})$, where $\nu = 1/2$ as above. That is, we observe linear scaling with corrections of order $N^{1/2}$ and smaller. The presence of the correction terms is consistent with behaviour expected from compact random walks, in contrast to the exact linear scaling which would obtain if the walks were free random flights. From the result $\xi \sim e^{1/p^2}$ in section 2.2, we expect to be able to conclude that $R_e^2 / N \sim e^{1/p^2}$. However, this is difficult to verify.
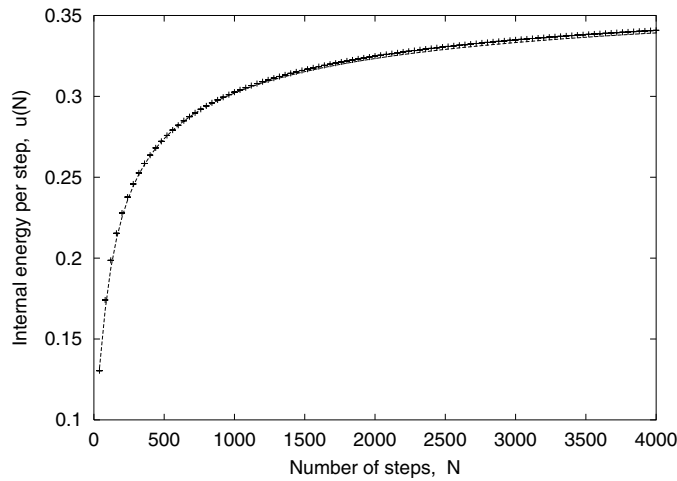
Figure 8. Scaling of internal energy per step, u, with path length, for trails with $p = 0.5$ open at length N, up to maximum length $N = 4000$. The line fitted has equation $u(N) = 0.38 - 2.69N^{-1/2} + 7.09N^{-1}$; the coefficients are accurate to two decimal places.

3.4. Internal energy

In the equilibrium model described in section 3.2, we may define the average internal energy U of a configuration of N steps by

$$\langle U \rangle = -\frac{\partial}{\partial \beta} \log \mathcal{Z}_N(w)$$

$$\sim -\frac{\partial}{\partial \beta} F_N(w) \tag{3.6}$$

since, up to constants, $F_N \sim \log \mathcal{Z}_N$. Since F_b and F_s in (3.3) are expected to be temperature dependent, taking the derivative of F with respect to temperature gives

$$u \sim u_b + u_s N^{-1/2} + \cdots \tag{3.7}$$

for the internal energy per step, U/N. Here, the corrections, which have carried through from the expression for free energy, are expected to be of the order of N^{-1}. The subscripts b and s denote bulk and surface terms, as previously.

We now compare these results with simulations conducted on the Manhattan lattice. Figure 8 shows data for internal energy per step, $u(N)$, generated from populations of open trails of length N steps at $p = \frac{1}{2}$. Application of a scaling form of the type given in (3.7) indicates that these kinetic trails exhibit behaviour consistent with the existence of a well-defined one-dimensional surface. We find the asymptotic behaviour $u \sim u_b \approx 0.38$, with $u_s \approx 2.7$, and as predicted, the corrections to the bulk and surface terms are of the order of N^{-1}. Since the bulk fractal dimension for these objects is $1/\nu = 2$, we conclude that kinetic self-avoiding trails on the Manhattan lattice are compact, rather than extended, with a form similar to that of a liquid droplet. This conclusion is supported by the scaling forms already presented for survival probability, end-to-end distance and radius of gyration. Although the above analysis was carried out for the particular case $p = \frac{1}{2}$, the same conclusions should hold for all trails away from the fixed point $p = 0$, since all trails generated at $p > 0$ belong to the same phase.

4. Conclusions and discussion

We have presented a model for quantum localization in class C, on the Manhattan lattice. The general results of [7] show that this may be mapped to a classical random walk problem, of trails with an attractive on-site interaction. The model depends on a single parameter p. A weak-coupling field-theoretic renormalization group analysis appropriate for small p, numerical results for moderate values of p, and a rigorous argument for $p > \frac{1}{2}$, all lead to the conclusion that for all $p > 0$ the walks almost always close after a finite number of steps, and correspond to compact objects with a typical linear size which is a monotonically decreasing function of p. As $p \rightarrow 0$, this size diverges like $\exp(\text{const}/p^2)$.

This picture leads to the conclusion that the quantum model on the Manhattan lattice is always in the localized phase, in contrast to the case of the L-lattice. This might have been expected, given the absence of edge states in the former case. We note that the weak-coupling RG equations for the classical walks have a critical dimension of 2, as is the case for Anderson localization. It would be interesting to compare the RG β-function along the attractor $u_2 = 2u_1$ with that obtained using sigma model methods [1]. This would involve relating our coupling u_2 to the conductance, which is the physical coupling of the sigma model approach.

The arguments above directly apply to the dynamic model of kinetic growth trails on the Manhattan lattice. However, an equivalence exists to a particular temperature of a (static) equilibrium statistical mechanical model of polymers on that lattice, namely self-interacting trails. Hence, the results allow us to conclude that this temperature lies in the collapsed phase of the equilibrium model. This is the first time a kinetic growth walk/trail model has mapped into such a phase.

There are several possibilities for extension of this work. The mapping established in [7] requires each node to have coordination number 4, with two incoming bonds and two outgoing bonds. This means that every node must either be of the type found on the L-lattice, where a random walker is required to make a turn either to the left or to the right, or of the Manhattan type, where the walker may either make a turn or continue straight on. In this paper, we have considered only graphs consisting of nodes of one type; however, one could also consider graphs consisting of an arrangement of nodes of both types. This work would be interesting in terms of both the quantum localization behaviour and the nature of the corresponding classical walks. In [7], Sp(4) bilayer systems were discussed, consisting of two coupled lattice layers each with Sp(2) symmetry. Work on Sp(4) models of this type is in progress [25]. In this vein, one could examine mixed bilayer systems, in which the upper and lower layers have different lattice structures. For example, the localization behaviour of a model with one L-lattice layer and one Manhattan lattice layer might be expected to differ from that of a system consisting of two L-lattice layers. The results presented in this paper and in [7] relate to models based in two dimensions. However, another possibility for further work would be to consider models whose underlying graphs are embedded in three or more dimensions. For example, in three dimensions, one could study a layered system, such as the three-dimensional U(1) model constructed by Chalker and Dohmen [26]. For systems in three or more dimensions, both insulating and metallic phases should exist; it is expected that each type of behaviour should hold over a range of values of p, with a transition from one to the other at some critical value $p = p_c$, where $p_c \in [0, 1]$. It would be interesting to discover whether this is indeed the case.

Acknowledgments

References

[1] Altland A and Zirnbauer M R 1997 *Phys. Rev.* B **55** 1142
[2] Kagalovsky V, Horovitz B and Avishai Y 1997 *Phys. Rev.* B **55** 7761
[3] Kagalovsky V, Horovitz B, Avishai Y and Chalker J T *et al* 1999 *Phys. Rev. Lett.* **82** 3516
[4] Gruzberg I A, Ludwig A W W and Read N 1999 *Phys. Rev. Lett.* **82** 4524
[5] Senthil T, Marston J B and Fisher M P A 1999 *Phys. Rev.* B **60** 4245
[6] Cardy J 2000 *Phys. Rev. Lett.* **84** 3507
[7] Beamond E J, Cardy J and Chalker J T 2002 *Phys. Rev.* B **65** 214301
[8] Chalker J T and Coddington P D 1988 *J. Phys. C: Solid State Phys.* **21** 2665
[9] Gunn J M F and Ortuno M 1985 *J. Phys. A: Math. Gen.* **18** 1095
    Ortuno M, Ruiz J and Gunn J M F 1991 *J. Stat. Phys.* **65** 453
[10] Ziff R M, Kong X P and Cohen E G D 1991 *Phys. Rev.* A **44** 2410
[11] Cao M S and Cohen E G D 1997 *J. Stat. Phys.* **87** 147
[12] Cohen E G D and Wang F 1995 *J. Stat. Phys.* **81** 445
[13] Peliti L 1984 *Phys. Rep.* **103** 225
[14] Amit D J, Parisi G and Peliti L 1982 *Phys. Rev.* B **27** 1635
[15] Obukhov S P and Peliti L 1983 *J. Phys. A: Math. Gen.* **16** L147
[16] Chalker J T Private communication
[17] Guttmann A J 1985 *J. Phys. A: Math. Gen.* **18** 567
[18] Guttmann A J 1985 *J. Phys. A: Math. Gen.* **18** 575
[19] Bradley R M 1989 *Phys. Rev.* A **39** 3738
[20] Bradley R M 1990 *Phys. Rev.* A **41** 914
[21] Owczarek A L and Prellberg T 1995 *J. Stat. Phys.* **79** 951
[22] Owczarek A L and Prellberg T 1998 *Physica* A **260** 20
[23] Owczarek A L, Prellberg T and Brak R 1993 *Phys. Rev. Lett.* **70** 951
[24] Hughes B D 1995 *Random Walks and Random Environments* vol 1 (Oxford: Oxford Science Publications)
[25] Beamond E J, Cardy J and Chalker J T (in preparation)
[26] Chalker J T and Dohmen A 1995 *Phys. Rev. Lett.* **75** 4496